The centrifugal microfluidic Bio-Disk platform. J. Micromech. Microeng. 17:S103–S115

ARTICLE *in* JOURNAL OF MICROMECHANICS AND MICROENGINEERING · JULY 2007

Impact Factor: 1.73 · DOI: 10.1088/0960-1317/17/7/S07

J. Micromech. Microeng. **17** (2007) S103–S115 doi:10.1088/0960-1317/17/7/S07

The centrifugal microfluidic Bio-Disk platform

Jens Ducrée[1,2], Stefan Haeberle[1], Sascha Lutz[1], Sarah Pausch[2], Felix von Stetten[2] and Roland Zengerle[1,2]

[1] HSG-IMIT, Wilhelm-Schickard-Str.10, D-78052 Villingen-Schwenningen, Germany
[2] IMTEK, Department of Microsystems Engineering, Georges-Koehler-Allee 106, D-79110 Freiburg, Germany

E-mail: jens.ducree@hsg-imit.de

Received 19 February 2007, in final form 17 April 2007
Published 28 June 2007
Online at stacks.iop.org/JMM/17/S103

Abstract
This paper reviews the centrifugal 'Bio-Disk' platform which is based on rotationally controlled, multi-scale liquid handling to fully integrate and automate complex analysis and synthesis protocols in the life sciences. The platform offers the crucial ingredients for a rapid development of applications: a coherent library of fluidic unit operations, a device technology for actuation, liquid interfacing and detection as well as a developer toolbox providing experimental testing, rapid prototyping and simulation capabilities. Various applications in the fields of life science, *in vitro* diagnostics and micro-process engineering are demonstrated.

(Some figures in this article are in colour only in the electronic version)

Introduction

Microfluidic lab-on-a-chip technologies have experienced a breathtaking surge over the last 10–15 years. The field started out from mere analytical separations—mainly chip-based chromatography and capillary electrophoresis as well as miniaturized (bio-)chemical sensors. However, it was recognized very early that, apart from a mere miniaturization, a comprehensive integration, automation and parallelization of upstream liquid handling is key for a successful commercialization of lab-on-a-chip systems. Therefore, different liquid handling platforms have been developed to implement unit operations such as sample take-up, sample preconditioning, reagent supply, metering, aliquoting, valving, routing, mixing, incubation, washing as well as analytical or preparative separations.

Contrasting the huge variety component technologies, techno-economically viable platforms typically have to severely restrict the number of technologies used for substrate fabrication, actuation and detection! The choice of the technology platform is hence governed by finding the best compromise between the mere analytical or preparative performance and issues such as liquid handling capabilities and manufacturability. Various application platforms have been proposed, among them electrokinetic systems [1], droplet-based electrowetting [2], large-scale integrated peristaltic systems [3] and hydrophobic venting [4]. This paper reviews a centrifugal microfluidic Bio-Disk platform which has been developed over the last years by IMTEK, HSG-IMIT and several partners [5].

Compared to other lab-on-a-chip platforms, we will elaborate at various occasions throughout this paper that the centrifugal approach offers a unique way to integrate liquid handling for sample preparation and subsequent detection. The process integration on a single substrate eliminates the need for an off-chip liquid handling by costly and error prone pipetting robotics. It will further be shown that many unit operations can be devised to operate widely independent from liquid properties such as viscosity, electrical conductivity, thermal behavior and even surface tension over a broad range of volumes. These unique features are particularly appealing to life science or *in vitro* diagnostic applications where volumes to be processed in the same test, e.g. sample and dilution buffer, often range on different orders of magnitude and the liquid properties are usually not exactly known and strongly diverge, e.g. of from sample to sample.

Our developments started out from previous academic and commercial efforts in this field of centrifugal microfluidics [6–24] which already came up with technologies featuring full-fledged workstations incorporating actuation, liquid interfacing and detection units as well as means for quality

control. Using proprietary substrate formats, these platforms have primarily focused on general chemistry testing and immunoassays using absorption, agglutination or fluorescence detection. Also the preparation of protein samples for subsequent analysis by MALDI-MS has been commercialized. For the rapidly emerging field of nucleic acid testing, key steps such as cell lysis, DNA isolation and thermocycling for polymerase chain reaction (PCR) have been realized. In the mid-term future, it seems feasible to integrate an entire process chain comprising all steps between the take-up of real-world samples to displaying the analytical result on a centrifugal microfluidic nucleic acid workstation.

Another branch of centrifugal microfluidics forks into the field of micro-process engineering. By making designated use of the frequency-dependent artificial gravity conditions and the pseudo-forces on the rotating substrate, applications such as ultra-fast mixing at high discharges, e.g. for chemical reacting, have been established. Also the centrifugally induced generation of multiphase systems such as highly monodisperse emulsions, segmented liquid–liquid and gas–liquid flow and air-to-liquid sampling has been shown [27].

The first section of this paper introduces the simple and robust centrifugo-hydrodynamic operating principles, allowing a liquid handling widely independent of the properties of the liquid. The next section surveys important unit operations for centrifugal-microfluidic liquid handling including the scope of so-far realized applications. After describing further constituents of the centrifugal microfluidic application platform, we conclude with a summary and outlook.

Centrifugal hydrodynamics

Forces

A fluid of mass density ρ on a planar substrate rotating at a distance r from a central axis at an angular velocity ω experiences the centrifugal force (density)

$$f_\omega = \rho r \omega^2 \tag{1}$$

the Euler force (density)

$$f_\mathrm{E} = \rho r \frac{\mathrm{d}\omega}{\mathrm{d}t} \tag{2}$$

scaling with the rotational acceleration $\mathrm{d}\omega/\mathrm{d}t$ and the Coriolis force (density)

$$f_\mathrm{C} = 2\rho\omega v \tag{3}$$

scaling with the fluid velocity v in the plane of the substrate (figure 1). In a centrifugal microfluidic system, these three forces can directly be controlled by the frequency of rotation $\omega = 2\pi\nu$.

Sedimentation and buoyancy

Due to the dependence of the centrifugal force on the density ρ(1), suspended particles or gas bubbles displacing a volume with the mass deviating by Δm from the substituted liquid experience a sedimentation or buoyancy force

$$F_g = \Delta m r \omega^2 \tag{4}$$

according to the sign of Δm in the artificial gravity field $g = r\omega^2$ (figure 2). The motion of the particle is counteracted by the viscous Stokes drag F_d.

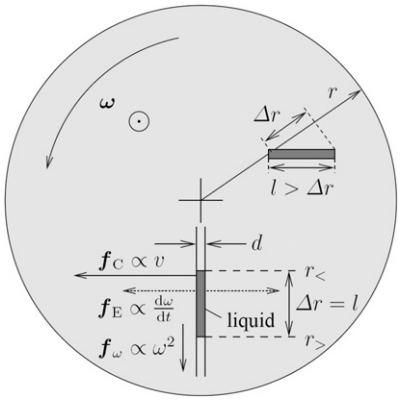

Figure 1. Geometry and forces on a disk spinning at the angular velocity vector $\vec{\omega}$ pointing out of the paper plane toward the reader. The radial coordinate is given by r. The liquid plug of diameter d and absolute length l extends between its inner and outer radial positions $r_<$ and $r_>$, respectively, with $\Delta r = r_> - r_<$ and $\bar{r} = 0.5\,(r_< + r_>)$. For a radially oriented plug, $\Delta r = l$, otherwise $\Delta r < l$. The liquid traveling at a speed $\vec{v}$ down the channel is exposed to the centrifugal force density $\vec{f}_\omega \sim \omega^2$ (1), the Euler force density $f_\mathrm{E} \sim \mathrm{d}\omega/\mathrm{d}t$ (2) and to the Coriolis force density $\vec{f}_c \sim v$ (3).

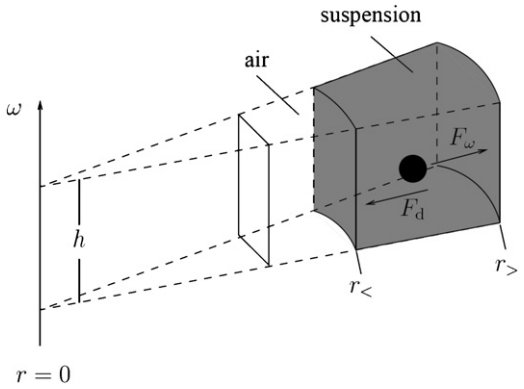

Figure 2. Sedimentation of a particle suspended in a liquid volume under the impact of a centrifugal field f_ω(1). The volume of height h is confined by the inner and outer radial boundaries $r_<$ and $r_>$, respectively. The motion of the particle follows the buoyancy corrected force f_ω accounting for the mass difference Δm between the particle and the displaced liquid volume. The centrifugal motion is counteracted by the viscous drag F_d.

Centrifugal flow

We consider the simplified case of a liquid plug in a straight and round radial channel of length Δr and diameter d at a mean radial position $\bar{r}$ [24, 38, 42]. Under the impact of the centrifugal force f_ω (1), a parabolic flow profile peaking at the center of the tube with a mean velocity

$$\bar{v} = \frac{\rho}{32\eta}\bar{r}d^2\omega^2 \tag{5}$$

establishes. Obviously, the overall discharge $Q = \bar{v}A \sim d^4$ is obtained from multiplying (5) with the channel cross section $A \sim d^2$.

The equivalent (external) pressure head

$$\Delta p_\omega = \rho\bar{r}\Delta r\omega^2 \tag{6}$$

corresponds to the pressure difference required to pump a pressure-driven flow at a mean velocity (5) through the same

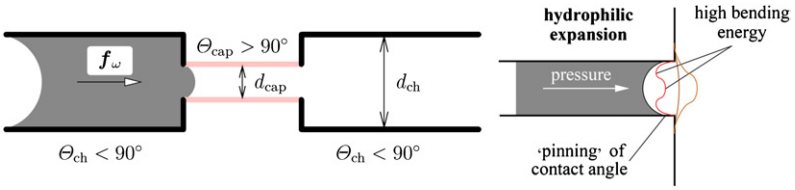

Figure 3. (Left) A hydrophobic valve is made up of a geometrical constriction from the channel diameter d_{ch} to a narrow capillary of diameter $d_{cap} \ll d_{ch}$. The contact angles are $\Theta_{cap} > 90° > \Theta_{ch}$. The capability to stop the flow up to a certain frequency threshold (8) is determined by the capillary pressure Δp_Θ scaling with the curvature d^{-1} as well as the inertia of the impinging flow. (Right) A hydrophilic barrier is represented by a sudden expansion. While still within the constriction near the exit of the channel, the 'pinning' of the contact angle as well as the constant channel width require a high transient curvature of the meniscus. This effect establishes an energetic barrier for the flipping of the meniscus from a concave to a convex shape, thus blocking the protrusion of the meniscus into the expansion up to a certain frequency of rotation.

channel. For the liquid with the characteristics of water ($\rho \approx 1000$ kg m^{-3}, $\eta \approx 1$ mPa s), a plug length $\Delta r = 2$ cm, a mean position $\bar{r} = 3$ cm and a channel diameter $d = 200$ μm, a mean velocity $\bar{v}$ of the order of 1 m s^{-1} (5) and a pressure head Δp_ω of about 20 kPa = 0.2 atm can be generated at a spinning frequency of 30 Hz (6). Note that the radial pressure distribution in a typical centrifugal flow may feature a pronounced minimum near the center of the channel. The dip originates from the centrifugally induced hydrostatic pressure increasing in the radial direction and the viscous pressure drop toward the outer end [24, 46].

Capillary priming

In centrifugal-microfluidic systems, it is often desirable to transport liquid toward 'back' the center of rotation. This is usually implemented by capillary action in narrow hydrophilic channels. The formula

$$t = \frac{4\eta l^2}{d\sigma \cos\Theta} \tag{7}$$

expresses the time t it takes a liquid with a surface tension σ a contact angle Θ, and viscosity η to fill a capillary of length l and diameter d of the circumferentially completely wetted capillary.

Capillary valving

A common means to effectuate valving in centrifugal microfluidics are narrow hydrophobic constrictions (figure 3, left). For the progression of the meniscus across a capillary barrier, a burst frequency

$$\nu\ (\mathrm{Hz}) = \frac{1}{\pi}\sqrt{\frac{\sigma|\cos\Theta|}{\rho\bar{r}\Delta r d}} \tag{8}$$

must be surpassed which is mainly governed by the surface tension of the liquid σ the contact angle Θ and the diameter d of the constriction [25, 26]. We roughly obtain $\nu \approx 20$ Hz for the liquid characteristics of water ($\sigma \approx 10^{-1}$ N m^{-1}), the above specified plug ($\bar{r} = 3$ cm, $\Delta r = 2$ cm), $d = 20$ μm and $\Theta = 120°$ (similar to water on Teflon). A capillary barrier can be regarded as a high-pass valve with respect to the frequency of rotation ω.

Also sudden expansions of hydrophilic channels work as capillary valves (figure 3, right). This is because the steep increase in the bending pressure dominates the creeping of the meniscus beyond sharp corner driven by the interfacial tension. While being pinned at the exit of the constriction, the surface tension counteracts a flipping from a concave to a convex meniscus which would lower the energetic barrier for passing the edge.

Siphoning

High-pass valving can be accomplished by a siphon structure under the impact of the artificial gravity $g = r\omega^2$ connected to the centrifugal field (figure 4). The siphon forwards the liquid as soon as the meniscus at $r_>$ has passed the crest point at r_{crest} and protruded further radially outward than the liquid level in the reservoir at $r_<$. In centrifugal-microfluidic systems, the priming of the exit channel is commonly implemented by capillary action while halting the rotation (7) or by adding a 'displacer liquid' [13, 14]. The siphoning flow stops once the liquid levels equilibrate hydrostatically at $r_< = r_>$ or once the continuity of the liquid column is disrupted.

Sacrificial valves

Destructible barrier layers are often employed to enable tasks such as vapor-proof valves for long-term onboard liquid storage. Liquids stored behind such sacrificial valves may be released by an external trigger working independent of the centrifugal field, e.g. by laser irradiation or mechanical punching of a pouch [13, 14]. By placing a number of sacrificial valves at alternative outlet vias, microfluidic networks can even be programmed on demand [21].

Centrifugal-microfluidic networks

The paradigm of liquid handling in most centrifugal-microfluidic systems concerns stepwise transitions between hydrostatic equilibria under the impact of rotationally induced artificial gravity. By opening a valve, the system becomes unbalanced to seek a new hydrostatic equilibrium where the center of gravity of the rotated liquid has advanced in radial direction.

Highly dynamic break-up phenomena which are common, for instance, in contact-free liquid dispensers, are quite uncommon in centrifugal microfluidic networks. This means that the liquid handling performance can be made widely independent of the flow properties, in particular the viscosity of the processed liquid. Within the chambers, centrifugally

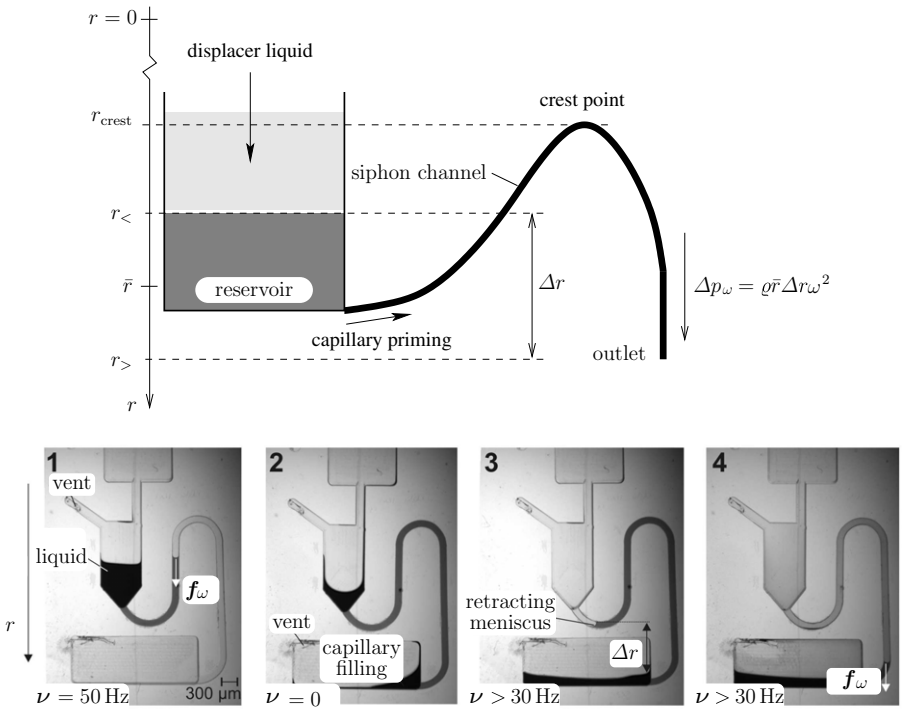

Figure 4. A siphon structure consists of a reservoir and an outlet which are connected by a completely liquid-filled tube passing the crest point r_{crest}. The radial boundaries of the liquid volume are $r_<$ and $r_>$. For $\Delta r = r_> - r_< > 0$, a flow propelled by the hydrostatic pressure $\Delta p_\omega \sim \Delta r$ (6) drains from the reservoir over the crest point to the outlet without an external pump. The siphon can either be triggered by a displacer liquid with subsequent rotation or by capillary priming of the hydrophilic channel at rest.

induced buoyancy efficiently supports the removal of gas bubbles from the liquid bulk.

Furthermore, the ability to supersede capillary and surface-tension-related forces by raising the frequency of rotation ω also means that undesirable effects can virtually be 'switched off'. This refers the transient suppression of unwanted capillary filling as, for example, implemented by a hydrophilically primed siphon (figure 4). Also the bending of surfaces in capillaries may be compensated by a strong centrifugal field, thus allowing us to shape flat menisci. The liquid-handling performance may hence be made widely independent of the surface tension σ.

Another ubiquitous topic in lab-on-a-chip technology is the parallelization of processes. The centrifugal field suggests to replicate identical structures according to the rotational symmetry in a spoke–wheel-like pattern. While such highly symmetric layouts have also been used in pressure-driven approaches with a single pump pressurizing a central feed channel, only the actuation by the centrifugal volume force suppresses 'hydrodynamic cross talk' between the parallel channels, e.g. the increase of the flow rate in a given channel due to the clogging of a neighboring channel.

In summary, the quasi-hydrostatic implementation of liquid handling under the impact of the frequency-controlled centrifugal field bears the potential to make liquid handling protocols widely independent of the liquid properties. The symmetry as well as the volume force nature of the centrifugal field also pave the road for a well-controllable parallelization of processes.

Centrifugal microfluidic operations

In this section, we outline the library of unit operations which can be concatenated on our novel centrifugal platform in order to implement integrated and automated liquid handling protocols.

Volume metering

Centrifugally induced liquid handling operations depend on the geometry (e.g. Δr) and the position (e.g. $\bar{r}$) of the processed liquid. An accurate volume metering is therefore not only essential for quantitative chemical analysis or synthesis, but also for a reproducible flow control in centrifugal microfluidic technologies.

Volume metering is predominantly realized by conceptually simple overflow principles (figure 5). The working principle can also be understood by picturing a filled bucket of known geometry. By drilling a first hole in the upper section of the bucket, gravity expels liquid until the meniscus reaches the lower edge of the hole. Another hole introduced into the lower section now issues a metered volume defined by the positions of the two lower edges. In centrifugal microfluidics, the first hole is usually an overflow to a waste while the second hole is represented by one of the previously introduced passive valving schemes, e.g. hydrophobic (figure 3, left) and hydrophilic barriers (figure 3, right) as well as siphons (figure 4) [28].

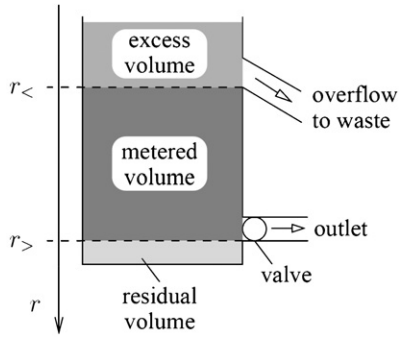

Figure 5. Metering by an overflow connected at a radially inward position $r_<$. As long as the valve blocking the exit channel at $r_>$ is closed, excess liquid depletes via the overflow to a waste. After the liquid surface has lowered to $r_<$, the lower valve is opened and a volume geometrically defined by $\Delta r = r_> - r_<$ is forwarded via the outlet to downstream structures. The valve can, for instance, be represented by a hydrophobic constriction (figure 3) or a hydrophilic siphon (figure 4).

Volume splitting

In case an initial volume has to be split into several (metered) aliquots, a hydrophilic zigzag structure with hydrophobic patches confining the conduits connected to each jag has been proposed (figure 6) [10, 29]. The upper jags are vents assuring pressure balance during the exit phase of the liquid. The outward pointing jags forward the geometrically defined volume retained in each 'V' to the downstream areas. Key factors for a proper functioning are a complete capillary priming of the zigzag, the compensation of boundary effects at the two laterally outermost 'Vs', as well as synchronous 'cutting' of the liquid column at the upper edges.

Batch-mode mixing

Mixing problems arise in microfluidic systems when the completion of diffusive mixing processes takes too long for a given application. For our rotating platform, we engineered an active mixing scheme complying with the modularity of our setup which is made up of two main units. The first unit is a disposable cartridge with passive components, the second is a device accommodating stationary components and a rotating engine which rests in the lab frame [30].

Mixing can be induced in a rotating chamber by rapid changes of the spinning frequency, i.e., a rotational acceleration $\mathrm{d}\omega/\mathrm{d}t$. The resulting Euler force f_E (2) leads to advective currents which appreciably speed up mixing (figure 7, left). The efficiency of the mixing process is primarily governed by the steepness of the frequency ramps $\omega(t)$ as well as by the geometry and the volume of the chamber. Due to the competition between favorable inertial effects and counteracting viscous dampening, chambers exceeding a height above 500 μm and displaying aspect ratios near unity are preferable for this 'shake-mode' mixing.

By introducing paramagnetic beads which are deflected by stationary permanent magnets aligned with alternating polarization along the orbit of the chamber, even a 'magnetic stirring' can easily be realized (figure 7, left). Compared to previous magneto-hydrodynamic mixing schemes using magnetic stirrer bars [31–33] or microparticles [34, 35] in an oscillating magnetic field, our scheme uses a stationary magnetic field with a rotating mixing chamber containing the actuators.

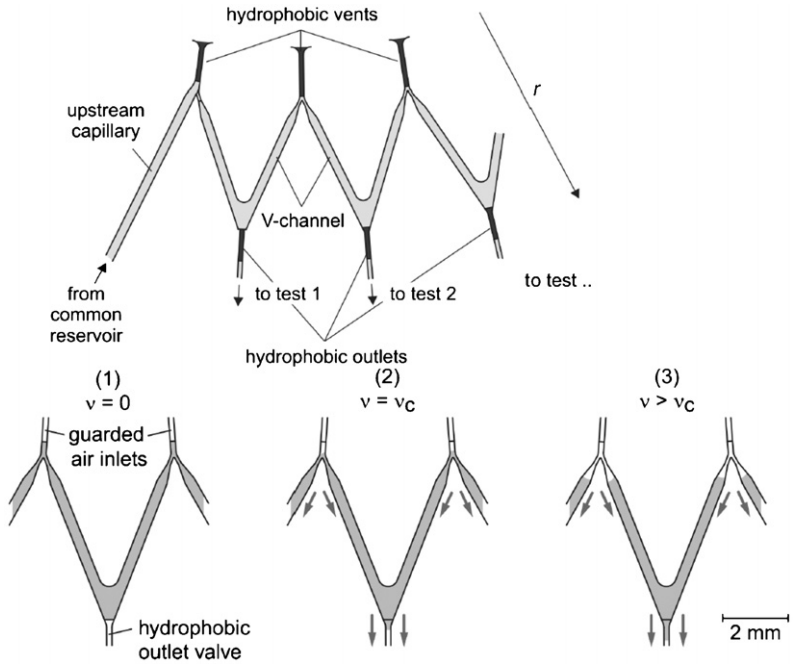

Figure 6. (Top) Schematic of the structure for parallel metering comprising a zigzag channel which features hydrophobically blocked valves and vents (functional principle described in [29]). (Bottom) By elevating the rotational frequency ω above the burst frequency of the outer hydrophobic barriers, the volume contained in each 'V' is released into attached test units. The precision of metering is linked to the symmetry of the break-up process.

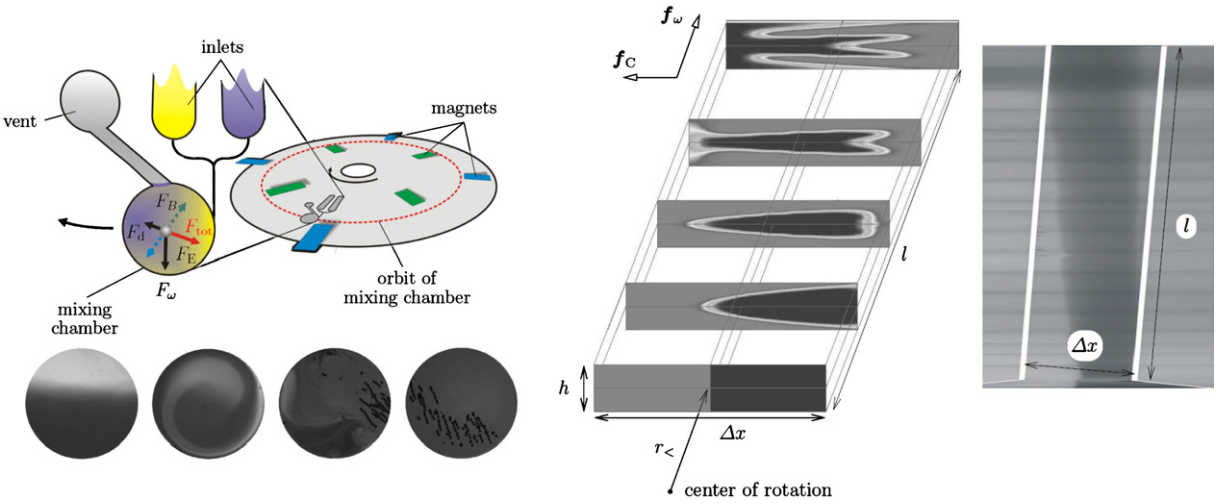

Figure 7. (Top left) Concept of the rotating microfluidic disk and the forces acting on a paramagnetic bead (adapted from [30]). A set of permanent magnets is aligned in the lab-frame at radial positions which are positioned inbound and outbound relative to the mean orbit followed by the rotating mixing chamber (dashed circle). Thus, a confined magnetic bead experiences an alternating radial force F_B deflecting the bead and induces advection via the viscous drag force F_d. The centrifugal force F_ω constantly points away from the center of rotation. Rapid changes of the sense of rotation lead to a Euler for F_E (2) on the bead and the liquid. (Bottom left) Flow patterns induced in the mixing chamber. (Right) Lateral spreading of two concurrent centrifugal flows A (clear) and B (dark) due to the Coriolis force f_C (3) for an angular frequency $\omega = 300$ rad s^{-1} in a rectangular radial channel of length $l = 2.1$ cm, height $h = 65$ μm and width $\Delta x = 320$ μm starting at $r_< = 3$ cm (adapted from [38, 39]). The right-hand side shows a top-view photography of the lateral spreading in the corresponding experiment. (Note that different length scales apply to the x- and y-axis.)

Mixing of flows

In case large 'macroscopic' volumes have to be mixed which cannot be contained in a single chamber or when the volumes are too small for implementing mixing effects based on the Euler force f_E (2), continuous-flow mixing schemes are applied. The aim is to contact the reagents with a large interfacial contact surface and short diffusion distances. A plethora of schemes to optimize micromixing between concurrent streams has been presented in the literature for pressure-driven flows [36, 37]. These schemes have often been enhanced by imposing secondary, transversal flow components or turbulent flow, e.g. via bends, impeller walls, grooves or stationary phases. The particular choice depends on parameters like the Reynolds number during operation and the constraints on the manufacturability and the required durability of the system.

Due to the similarity of the flow profiles, most of these passive, continuous-flow schemes can, in principle, also be adopted for centrifugally driven flows. In addition, the availability of the Coriolis pseudo-force f_C (3) offers an intrinsic means for the generation transversal flow components, even in straight radial channels exhibiting a constant cross section (figure 7, right). It can be shown that the scaling of the force ratio f_ω/f_C follows ω^{-1} [38, 39], such that the Coriolis-force induced mixing is most efficient toward high frequencies of rotation ω. This allows us to combine high mixing quality with high flow rates of the order of 1 ml s^{-1}! Also options for an online flow control have been demonstrated [40].

Routing

The routing of a sequence of discrete volumes to designated outlets is a common task, e.g. in preparative protocols where sample, wash and elution buffers have to be directed to the waste or a receiving vessel after passing a common stationary phase. While different strategies such as flow focusing concepts have been pursued for lab-on-a-chip systems, we here address concepts connected to the rotational motion of centrifugal microfluidic systems.

In the first approach in figure 8 (left), the incoming liquid stream disintegrates at the orifice on the upper left side of a large chamber [17, 41]. The individual droplets preferentially stick to the left-hand wall where the centrifugal field guides them toward a hydrophobic patch at the entry of the first outlet channel. At high frequencies of rotation ω, the droplets overcome the capillary barrier. At lower frequencies ω, the interfacial force supersedes the centrifugal field to deflect the droplet toward the second outlet on the right-hand side of the chamber.

Another routing scheme presented in figure 8 (right) is primarily based on the Coriolis force f_C (3). In an inverse Y-channel geometry, the common radial inlet splits into two symmetric outlets [42, 43]. As the Coriolis force f_C prevails the centrifugal force f_ω toward elevated frequencies of rotation ω a critical frequency ω^* exists above which mere digital switching occurs. Ideally, individual droplets pass the chamber interspersed between the inlet and the outlets in a free flight. The performance of this 'Coriolis switch' is tightly linked to the dimensions and surface properties of the channels and the chamber. Attachment to the upper and lower walls by capillary forces tends to deteriorate the performance of binary switching. Note that a similar switching behavior could also be achieved by (solely or additionally) using the Euler force f_E (2).

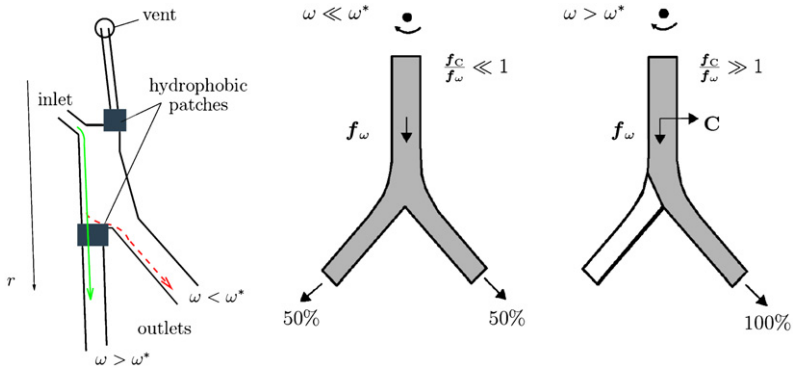

Figure 8. Liquid routers. (Left) Liquid is introduced via the upper left inlet and follows the left-hand chamber walls toward a hydrophobic region at the entrance of the first outlet (working principle introduced by Gyros AB [17] in [41]). Depending on the centrifugal field and thus the frequency ω, the droplet can either pass the capillary barrier or proceed to the second outlet. (Right) Flow through a symmetric, inverse Y-structure (adapted from [42, 43]). (Right) At low frequencies ω where the Coriolis force f_C (1) is still negligible compared to f_ω (2), the flow is symmetrically split between both outlets. As the Coriolis force f_C dominates beyond a critical frequency ω^*, it diverts 100% of the flow into an outlet addressed by the sense of rotation.

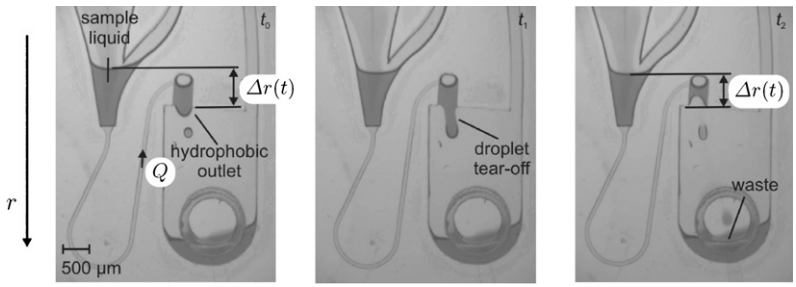

Figure 9. Course of liquid break-off at the hydrophobic outlet of the drain channel in a structure designed to stabilize the flow rate Q (5). The liquid tears off into a waste reservoir. This way, the outer radial position of the liquid plug $r_>$ is kept constant. The variation of inner plug position $r_<$ is minimized by the large lateral extension of the upstream chamber.

Control of flow rate

The centrifugally driven flow rate is governed by the mean radial position $\bar{r} \sim [r_< + r_>]$ (5) of the liquid volume and the frequency of rotation ω. In typical assay protocols, a metered volume such as a reagent or a wash buffer is driven from an upstream chamber by the centrifugal force through a stationary phase such as a biosensitive layer immobilized on the channel wall, aggregated beads or a membrane.

In many cases, the variation of the flow velocity due to changes in $\bar{r}$ during the depletion of the upstream chamber ought to be minimized to homogenize incubation times. Looking at (5), the flow velocity can be stabilized by an online adjustment of ω. Such a dynamic adjustment of ω either requires a very well reproducible flow behavior or a closed loop control of $\bar{r}$, e.g. via continuous tracking of the transient positions of the menisci $r_<$ and $r_>$.

An alternative to the adjustment of ω is to pinpoint $r_<$ and $r_>$ as far as possible during the flow interval. Regarding the downstream end at $r_>$, the continuous liquid column can, for example, be disrupted at a hydrophobic orifice leading into a large receiving vessel (figure 9). The fixed radial position of the orifice then coincides with $r_>$. For the upstream meniscus, the radial change of the inner meniscus $r_>$ can be minimized by maximizing the lateral dimensions of the issuing reservoir.

For other applications such as the simultaneous sedimentation at large ω see below, the overall minimization of the flow rate Q may be required. Using $Q \sim d^4$ (5), $\Delta p_\omega \sim \Delta r$ (6) and a hydrodynamic resistance proportional to the channel length l, we can also reduce the quotient $\Delta r d^4/l$ to throttle the flow rate. This geometric factor reflects the ratio of the hydrostatic pressure head ($\sim\Delta r$) to the hydrodynamic resistance ($\sim l/d^4$). So a radially shallow channel with a high tilt angle between the channel axis and the radial direction, i.e. $\Delta r \ll l$, diminishes Q. A further reduction of Q can be accomplished by increasing the flow resistance, e.g. by a narrow, meander-like flow channel with an embedded stationary phase.

Centrifugo-magnetic pumping

The production and handling of liquid–gas systems is a common task of multiphase lab-on-a-chip systems. The surface-tension stabilized bubbles are often employed as spacers between different droplets in so-called plug-flow schemes. However, for the introduction of the gas phase in a liquid stream requires a differential pressurization of the gas.

We therefore developed a centrifugo-magnetic pumping scheme which well complies with the modular paradigm of the rotating system (figure 10). Two flat and round magnetic plates are incorporated into an elastomer sealing above a valve chamber and an adjacent pump chamber [44]. This actuation scheme resembles the previously introduced 'magnetic PDMS' membranes deflected by electromagnets for

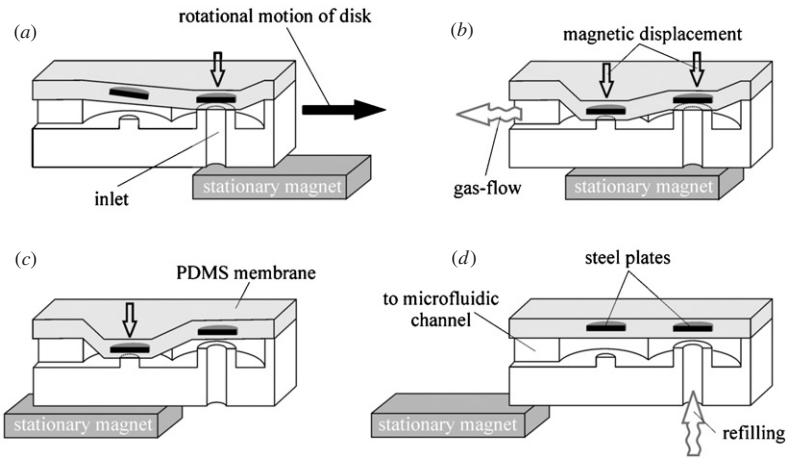

Figure 10. Functional principle of the gas micropump (reprinted from [44]). The pump chamber orbits above a stationarily mounted permanent magnet. The two steel plates within the PDMS lid are spaced at a defined azimuthal distance to induce a sequence of displacements during rotation for pressurizing the gas. After the magnet has passed, the chambers are primarily replenished by ambient gas through the inlet of the valve chamber.

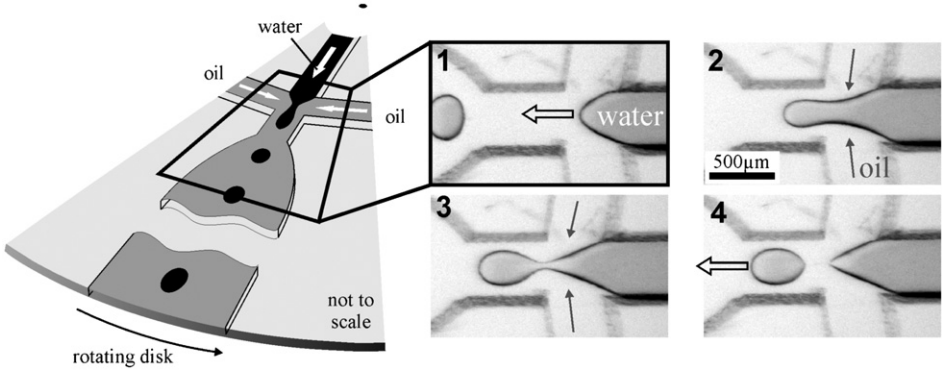

Figure 11. Centrifugal droplet generation ([46], with permission from Springer Science and Business Media). The dispersed phase is contacted from both sides with the continuous phase at the junction of a flow-focusing structure. The main impact parameters are the three incoming flow rates, the angle at which the side flows impact the central stream and the radial position of the intersection. The droplet generation is characterized by the droplet diameter, the droplet spacing, and the droplet rate.

static setups [45]. While rotating, the magnets in our rotary scheme are sequentially deflected upon passing a stationary permanent magnet positioned at the orbit to differentially pressurize the gas. The pumping is impacted statically by the chamber geometry, the elastic modulus of the sealing and the magnetic force as well as dynamically by the spinning rate corresponding to the actuation frequency.

Droplet generation

Several means to generate liquid droplets by centrifugal microfluidic technologies have been investigated. In a first concept, a liquid plug is issued at a central orifice and cut off by two constricting flows exhibiting transversal components (figure 11) [46].

The other scheme is based on a dispenser delivering individual droplets from a nozzle through an intermediate air spacer into a receiving liquid (see later in figure 16, left) [47]. While conventional dispensing schemes such as inkjet technologies require a highly dynamic ejection for surpassing the surface tension and viscosity, the centrifugal droplet generation is associated with the frequency-scalable artificial gravity field virtually 'pulling out' the droplet from the nozzle.

As the rotational motion is even stabilized by the inertia of the rotor, these centrifugal schemes are intrinsically pulse-free and thus highly reproducible. We could experimentally show the production of highly monodisperse emulsions.

Particle sedimentation

An initially homogeneous particle suspension separates in the presence of a centrifugal field. The speed of sedimentation is governed by the difference of the masses of the particle and the displaced liquid Δm as well as the Stokes drag F_d scaling with the radius, the viscosity and the velocity of the particle (figure 2). A phase boundary, the so-called shock interface travels from the inner liquid interface toward the outer perimeter of the vessel. As the rotary drive offers the function of a customary centrifuge, also sedimentation processes can be enforced. Thus is, for instance, implemented by the cell volume fraction in whole blood (hematocrit) measurement displayed in figure 12 [48, 49].

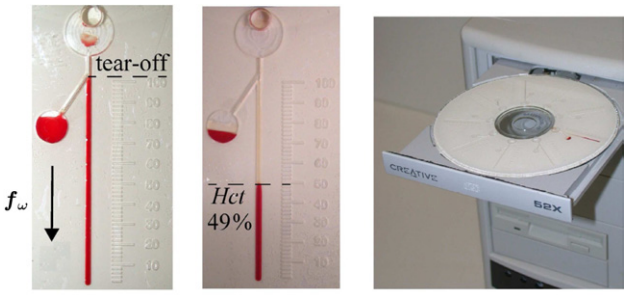

Figure 12. Centrifugal hematocrit determination [48, 49] (adapted from [48], [49] reproduced with permission from Springer Science and Business Media). (Left) After an unmetered volume of whole blood is applied to the inlet reservoir, the capillary is primed and a precise volume of whole blood is metered during rotation. (Center) Following sedimentation, the absolute hematocrit can be determined with the calibrated scale imprinted along the channel. (Right) It has been demonstrated that this test can even be performed on a standard CDROM-drive.

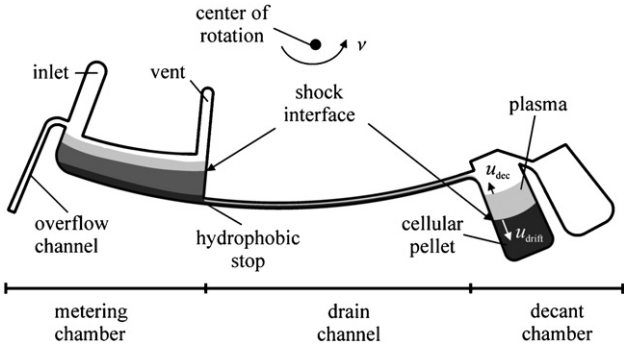

Figure 13. Flow scheme of a decanting structure for plasma separation from whole blood (adapted from [50]). A metered volume of the blood sample is defined between hydrophobic stop and overflow channel. Upon breaking the outlet valve, a metered volume flows via the drain channel into the decant structure. A shock interface separating plasma from the cellular pellet builds out in all parts of the network and proceeds radially outward at a speed u_{drift}. The filling height of the decant chamber rises at counter-current speed u_{dec} before the plasma overflows into the plasma collection chamber. The speed u_{dec} of the filling height in the cell reservoir is adjusted by the hydrodynamic resistance of the drain channel so that only purified plasma advances to the plasma reservoir.

However, in typical applications based on centrifugal microfluidics, the sedimentation only constitutes one upstream unit step in an integrated process chain to which the supernatant (or the concentrated pellet) has to be forwarded. Figure 13 shows an integrated sedimentation structure based on hydrophobic valving for the initial, overflow-based metering. Next, a radially flat and narrow transfer channel throttles the flow such that the suspension has sufficient time to sediment in the separation chamber before pure supernatant is passed on to the plasma chamber [50]. From there, the plasma can, e.g., be forwarded to downstream structures by a hydrophilic capillary while halting the rotation. The alternative siphon-based, batch-mode metering and sedimentation structure in figure 14 works without hydrophobic surface patterning and without a long throttle channel to save precious on-disk space [28].

We also explored a centrifugal sedimentation of particles under the impact of a transversal dielectrophoretic (DEP) deflection [51–53]. The DEP force field is built up by onboard electrodes, electronics and batteries, thus allowing a two-dimensional separation according to the density and dielectrophoretic properties of the particle, e.g. a sorting of dead and viable cells into distinct exit channels [54].

Polymer microfabrication

We established a polymer prototyping chain for the structuring, surface modification and sealing of the substrates [55]. The method is closely derived from the well-known ‘soft lithography’ approach elaborated by the Whitesides group [56]. For subsequent polymer mass fabrication, various technologies are available such as injection molding are available [57]. First, an intermediate master is made by multi-layer SU-8 or dry etching technology using laser-printed foils. This original mold is then transferred by PDMS casting into a flexible and thus easily demoldable master for hot embossing (‘soft embossing’).

Alternatively, the casting into an epoxy material has proven to supply a sufficiently stable master for small lot injection molding [58]. This epoxy casting approach saves time and costs compared to traditional, high-performance processes based on LIGA [59].

After the structuring of the bulk material, postprocessing such as surface modification (e.g. hydrophilic, hydrophobic, biosensitive, anti-fouling), sealing (e.g. thermal bonding, gluing), integration of stationary phases (e.g. aggregated beads, membranes) and reagent loading (e.g. lyophilized, liquid storage in pouch) may be required.

Device technology

The modular approach of our centrifugal microfluidic platform consists of a multi-purpose device which operates the passive microfluidic disk. The device is equipped with a set of lab-frame components to realize a comprehensive group of applications (figure 15, left). A frequency-controlled motor and a holder for the rotating substrates (e.g. disks) constitute the core elements of the device. Depending on the application, liquid, optical and possibly electrical interfacing between rotating ‘on-board’ components and stationary ‘lab-frame’ components such as contact-free dispensers or detection units can be incorporated. A process control software synchronizes events such as liquid handling or optical readout to the periodic motion of the substrate.

Rotor and cartridge formats

Due to its rotational symmetry, the generic format for a centrifugal microfluidic substrate is a disk. However, the disk shape may for various reasons not fit to the envisioned application. This may be due to the established standard substrate in the application field which complies with up- or downstream instrumentation. Also cost reasons may interfere with the disk shape, e.g. when a one-test-per-substrate

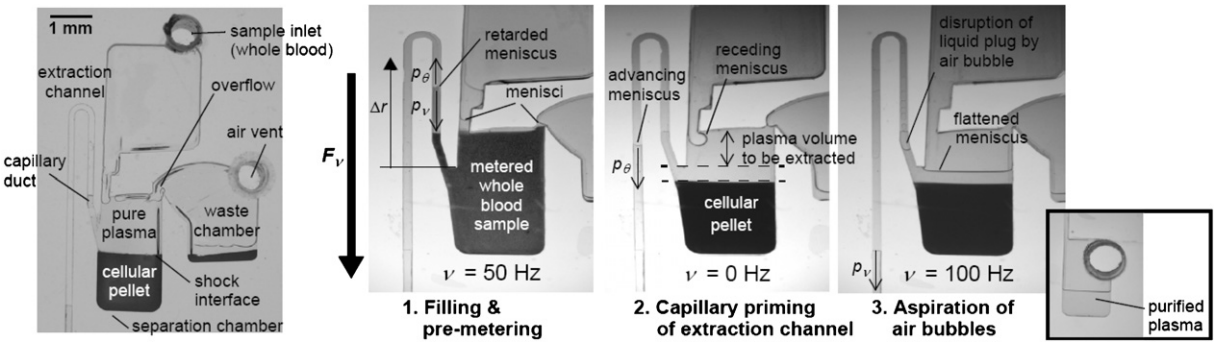

Figure 14. Section view of the plasma extraction structure (adapted from [28]). (1) After injection through the inlet, a droplet of raw blood is metered by the overflow channel. Three menisci can be identified in the inlet and both outlets. (2) The cells settle towards the bottom of the reservoir as the shock interface separating pure plasma and cellular blood proceeds. Once the shock interface is below the inlet of the plasma extraction channel, the disk is stopped and the extraction channel is filled by the capillary pressure p_θ. (3) A net radial offset $\Delta r < 0$ induces centrifugal pressure p_ω to pump the plasma through the extraction channel. The extraction process ceases at the point when air is sucked into the plasma extraction channel. This point is reproducibly defined (CV $< 1\%$) by the centrifugally supported flattening of the meniscus towards high spinning frequencies. The extracted plasma is collected in a reservoir attached to the extraction channel for further use.

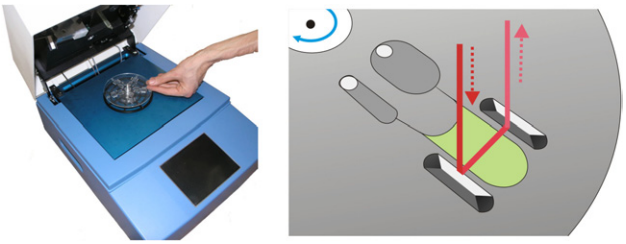

Figure 15. (Left) Bio-Disk analyzer. (Right) Absorption measurement by optical beam guidance using total internal reflection at substrate-integrated V-grooves on the Bio-Disk analyzer (adapted from [61, 62]).

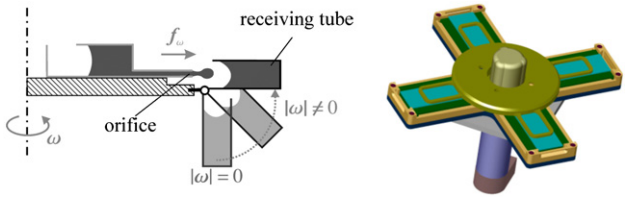

Figure 16. Different rotor and substrate formats for centrifugal microfluidic technologies. (Left) Liquid droplets are issued in a contact-free fashion from the side surface of the cartridge into a standard reaction tube aligning according to the centrifugal field (adapted from [47]). (Right) Rotor accommodating standard microscope (microarray) slides (adapted from [60]).

paradigm is mandatory in diagnostic applications to avoid cross-contamination.

We have constructed different rotors for the Bio-Disk technology to assure compatibility with established formats. Figure 16 (left) shows a rotor which has been adapted for the purification and extraction of nucleic acid on the analogy of common spin-column protocols [47]. A sequence of sample and different buffer solutions is loaded to the disk and routed by the Coriolis force to a distinct outlet selected by the sense of rotation (figure 8, left). To allow a seamless integration into the process flow in the lab, the purified DNA is expelled in a free jet through orifices in the side surface of the disk into standard Eppendorf tubes. The receiving tubes are accommodated in a 'flying bucket' extension of the rotor to freely align according to the ratio of gravity and the centrifugal force in order to avoid spill over.

Another example is the centrifugal microarray processor illustrated in figure 16 (right) [60]. The novel rotor can be loaded with four standard microarray slides which are clamped against an elastomeric PDMS inlay featuring microfluidic structures. Using the shake-mode protocol (figure 7, left), incubation and washing of the microarray can be performed very efficiently in a flat flow chamber above the microarray. A siphon structure (figure 4) at the outlet of the chamber allows a well-controlled displacement of a processing buffer by the subsequent buffer into a waste reservoir such that the microarrays never run dry.

Optical detection

Most common detection methods, such as qualitative test strips or highly sensitive fluorescent measurements, in analytical or diagnostic assays are based on optical techniques. Among other detection concepts, these contact-free optical principles are also most compatible with the modular paradigm of the centrifugal platform. This section reviews several optical detection schemes which have already been successfully implemented on the Bio-Disk platform.

Visual inspection. The simplest, 'detector-free' scheme is visual inspection. Combining microstructures with designated frequency protocols, we successfully demonstrated the implementation of hematocrit (cell volume ratio in whole blood) and agglutination-based blood-group testing on a simple disk centrifuge or even on an ordinary CDROM-drive (figure 12) [48, 49].

Absorption measurements. In clinical chemistry, the detection of many blood parameters is based on optical absorption. Toward decreasing optical densities, the obtainable sensitivity is limited by the short optical path lengths immanent to microscopic volumes. In addition, the volumes are commonly contained in flat chambers which can only be probed through the flat top side.

To tackle this problem, we elaborated an optical guidance based on the total internal reflection at polymer–air interface of V-grooves incorporated the backside of the substrate (figure 15, right) [61–63]. Under perpendicular incidence, the beam is deflected by 90° into the plane of the substrate to probe the measurement chamber. Another V-groove then redirects the attenuated beam toward the stationary detector. This way, the optical path length through the flat measurement chamber and thus the performance of the measurements are massively enhanced compared to direct (perpendicular) beam incidence. The achieved sensitivity has proven to be comparable to standard colorimetric, cuvette-based assays such as alcohol, glucose and hemoglobin levels in serum and whole blood [64, 65]. It has also been shown that several different parameters can be measured at the same run on the same disk in parallel to form so-called disease panels.

Chemiluminescence measurements. We implemented a parallel readout technique for running common chemiluminescent assay formats on our centrifugal microfluidic platform [66]. The pilot application was a panel of cardiac markers. Antigens indicating an acute myocardial infarction (AMI) were captured by a bead-based chemiluminescent ELISA procedure conducted under rotation on a polymer disk and detected by a photomultiplier (PMT). Parallel channel structures allow the quasi-simultaneous screening for different markers. However, a clear disadvantage of the readout under rotation is the immanent discontinuity of photon acquisition.

Fluorescence detection. We also evaluated schemes for bead-based fluorescence detection [67–69]. On the one hand, the detection on a bead phase allows us to introduce the sensitive capture molecules after the sealing of the substrate, possibly requiring thermally and/or chemically harsh conditions. This also makes the disk reconfigurable. On the other hand, the flow through a stationary phase allows rapid and tightly controlled reaction conditions. Furthermore, detection in a single channel can be multiplexed, e.g. by a color-encoding of off-disk prepared beads. The color encoding can, for instance, be implemented by incorporation of quantum dots or dyes into the beads.

Test and development stand

For the development of centrifugal microfluidic technologies, it is very useful to capture the dynamic processes during high-speed rotation. We devised a stroboscopic measurement setup comprising a microscope mounted CCD camera with a short exposure time and a flash light which are synchronized to the rotational motion as well as a GUI for setting frequency protocols and frame grabbing parameters [70].

Summary and outlook

In this paper, we have outlined the simple, robust and well-controllable operational principles of centrifugal microfluidics. Most liquid handling functions can be implemented by the interplay between frequency-controllable inertia (centrifugal force, Euler force, Coriolis force), capillary action (hydrophilic/hydrophobic) and fluidic structures on the micro- to milli-scale. The paramount features of our centrifugal technology are as follows.

- Modular setup:
  - centrifuge drive—passive microfluidic substrate,
  - easy exchange of disposable cartridge,
  - flexibility of substrate formats (disk, slide, etc).
- Centrifugal field:
  - pulse-free pumping,
  - no pressure-tight interfaces needed,
  - low pressure load on lids,
  - standard operation in sample prep,
  - robust liquid handling widely decoupled from viscosity and surface tension,
  - intrinsic, buoyancy-based bubble removal,
  - Coriolis force manipulates flows,
  - many laboratory protocols rely on centrifugation,
- Rotational symmetry:
  - replication of identical process channels,
  - simultaneous processing of parallel channels,
  - sequential channel-by-channel processing,
  - excellent temperature homogeneity.
- Full process integration and automation.

Note that most conventional lab-on-a-chip technologies may, in principle, be transferred to the ‘lab-on-a-disk’, in particular when they are active only while halting the rotation. The above-listed benefits have to be carefully weighed against potential drawbacks.

- Interfacing with lab-frame components:
  - pipettes and dispensers,
  - quality control units,
  - detection units.
- On-board components:
  - exposure to centrifugal force,
  - need for mechanical balancing,
  - difficult wiring, e.g. for electrical power, liquids and signal transmission,

which are primarily associated with the rotating motion of the substrate.

Several companies have, had or are slated to have commercial activities based on centrifugal microfluidic technologies [14, 17, 19–21]. It is expected that researchers will continue to further augment the level of process integration, automation, parallelization and miniaturization. Multi-purpose workstations which can run a set of different applications, each represented by a designated substrate (disk), will certainly be a strong selling point. The largest markets for centrifugal microfluidic technologies are expected for decentralized systems for high-sensitivity medical diagnostics and (bio-)chemical analysis as well as research tools for pharmaceutical drug discovery.

Apart from reliability, sensitivity, interfacing with established standards and regulatory issues, the main hurdle to pass for a successful commercialization is clearly the price per assay or preparation compared to presently established or other emerging technologies. This concerns the polymer substrate as well as the device for which important lessons

may, for instance, be learnt from the massive cost erosion of Compact Disc™ technology over the last decades. Patients autonomously performing complex diagnostic assay protocols by simply introducing a body liquid into a 1-$ disk which is automatically 'played' by a 10-$ discman remains a truly tantalizing vision for centrifugal-microfluidic technologies.

References

[1] Harrison D J, Fluri K, Seiler K, Zhonghui F, Effenhauser C S and Manz A 1993 Micromachining a miniaturized capillary electrophoresis-based chemical analysis system on a chip *Science* **261** 895–7

[2] Lee J and Kim C-J 2000 Surface-tension-driven microactuation based on continuous electrowetting *J. Microelectromech. Syst.* **9** 171–180

[3] Unger M A, Chou H-P, Thorsen T, Scherer A and Quake S R 2000 Monolithic microfabricated valves and pumps by multilayer soft lithography *Science* **288** 113–6

[4] Hosokawa K, Fujii T and Endo I 1999 Handling of picoliter liquid samples in a poly(dimethylsiloxane)-based microfluidic device *Anal. Chem.* **71** 4781–5

[5] Bio-Disk project www.bio-disk.com

[6] Schembri C T, Ostoich V, Lingane P J, Burd T L and Buhl S N 1992 Portable simultaneous multiple analyte whole-blood analyzer for point-of-care testing *Clin. Chem.* **38** 1665–70

[7] Madou M J and Kellogg G J 1998 LabCD: a centrifuge-based microfluidic platform for diagnostics *Systems & Technologies for Clinical Diagnostics & Drug Discovery; Proc. SPIE* **3259** 80–93

[8] Madou M, Zoval J, Jia G, Kido H, Kim J and Kim N 2006 Lab on a CD *Annu. Rev. Biomed. Eng.* **8** 601–28

[9] Gustafsson M, Hirschberg D, Palmberg C, Jörnvall H and Bergman T 2004 Integrated sample preparation and MALDI mass spectrometry on a microfluidic compact disk *Anal. Chem.* **76** 345–350

[10] Inganäs M, Dérand H, Eckersten A, Ekstrand G, Honerud A-K, Jesson G, Thorsén G, Söderman T and Andersson P 2005 Integrated microfluidic compact disc device with potential use in both centralized and point-of-care laboratory settings *Clin. Chem.* **51** 1985–7

[11] Pugia M J, Blankenstein G, Peters R-P, Profitt J A, Kadel K, Willms T, Sommer R, Kuo H H and Schulman L S 2005 Microfluidic tool box as technology platform for hand-held diagnostics *Clin. Chem.* **51** 1923–32

[12] Anderson N G 1969 Computer interfaced fast analyzers *Science* **166** 317

[13] Schembri C T, Burd T L, Kopf-Sill A R, Shea L R and Braynin B 1995 Centrifugation and capillarity integrated into a multiple analyte whole-blood analyzer *J. Autom. Chem.* **17** 99

[14] Abaxis www.abaxis.com

[15] Madou M J and Kellogg G J 1998 *Systems & Technologies for Clinical Diagnostics & Drug Discovery; Proc. SPIE* **3259** 80–93

[16] Duffy D C, Gillis H L, Lin J, Sheppard N F and Kellogg G J 1999 Microfabricated centrifugal microfluidic systems: characterization and multiple enzymatic assays *Anal. Chem.* **71** 4669–78

[17] Gyros Microlabs www.gyros.com

[18] Inganäs M, Dérand H, Eckersten A, Ekstrand G, Honerud A-K, Jesson G, Thorsén G, Söderman T and Andersson P 2005 Integrated microfluidic compact disc device with potential use in both centralized and point-of-care laboratory settings *Clin. Chem.* **51** 1985–7

[19] Tecan www.tecan.com

[20] EAT—Eppendorf Array Technologies www.eppendorf.com/eat/en/

[21] SpinX Technologies www.spinx-technologies.com

[22] Sakurai T, Uchida K, Kuno N and Nagaoka Y 2005 Development of nucleic acid extraction technology and its product strategy *Hitachi Rev.* **54** 70–3

[23] Felton M 2003 CD simplicity *Anal. Chem.* **75** 302A–306A

[24] Kim D S and Kwon T H 2006 Modeling, analysis and design of centrifugal force-driven transient filling flow into a circular microchannel *Microfluid. Nanofluid.* **2** 125–140

[25] McNeely M R, Spute M K, Tusneem N A and Oliphant A R 1999 Hydrophobic microfluidics *Microfluidic Devices & Systems: II; Proc. SPIE* **3877** 210–20

[26] Ekstrand G, Holmquist C, Edman Örlefors A, Hellman B, Larsson A and Andersson P 2000 Microfluidics in a rotating CD *Proc. Micro Total Analysis Systems Symp. (μTAS 2000) (Enschede, The Netherlands, 14–18 May)* ed A van den Berg, W Olthuis and P Bergveld (Dordrecht, The Netherlands: Kluwer Academic) pp 311–4

[27] Haeberle S, Brenner T, Schlosser H-P, Zengerle R and Ducrée J 2005 Centrifugal micromixer *Chem. Eng. Technol.* **28** 613–616

[28] Steigert J, Brenner T, Grumann M, Riegger L, Lutz S, Zengerle R and Ducrée J 2007 Integrated siphon-based metering and sedimentation of whole blood for centrifugally integrated colorimetric assays *Biomed. Microdev.* at press

[29] Andersson P and Ekstrand G 2003 Retaining microfluidic microcavity and other microfluidic structures *Patent Application* WO03018198 (Gyros AB)

[30] Grumann M, Geipel A, Riegger L, Zengerle R and Ducrée J 2005 Batch-mode mixing with magnetic beads on centrifugal microfluidic platforms *Lab on a Chip* **5** 560–65

[31] Lu L-H, Ryu K S and Liu C 2002 A magnetic microstirrer and array for microfluidic mixing *J. Microelectromech. Syst.* **11** 462–9

[32] Mensing G A, Pearce T M, Graham M D and Beebe D J 2004 An externally driven magnetic microstirrer *Phil. Trans. R. Soc.* A **362** 1059–68

[33] Ryu K S, Shaikh K, Goluch E, Fan Z and Liu C 2004 Micro magnetic stir-bar mixer integrated with parylene microfluidic channels *Lab on a Chip* **4** 608–13

[34] Rida A and Gijs M A M 2004 Dynamics of magnetically retained supraparticle structures in a liquid flow *Appl. Phys. Lett.* **85** 4986–8

[35] Rong R, Choi J and Ahn C 2003 A novel magnetic chaotic mixer for in-flow mixing of magnetic beads *Proc. 7th Int. Conf. on Micro Total Analysis Systems (μTAS 2003) (Squaw Valley, Ca, 5–9 Oct.)* ed M A Northrup, K F Jensen and D J Harrison pp 335–8

[36] Hardt S, Drese K S, Hessel V and Schönfeld F 2005 Passive micromixers for applications in the microreactor and μtas fields *Microfluid. Nanofluid.* **1** 108–118

[37] Nguyen N-T and Wu Z 2005 Micromixers—a review *J. Micromech. Microeng.* **15** R1–16

[38] Ducrée J, Haeberle S, Brenner T, Glatzel T and Zengerle R 2005 Patterning of flow and mixing in rotating radial microchannels *Microfluid. Nanofluid.* **2** 97–105

[39] Ducrée J, Brenner T, Haeberle S, Glatzel T and Zengerle R 2005 Multilamination of flows in planar networks of rotating microchannels *Microfluid. Nanofluid.* **2** 78–84

[40] Haeberle S, Zengerle R and Ducrée J 2005 Online process control for centrifugal microfluidics *Proc. 13th Int. Conf. on Solid-State Sensors, Actuators & Microsystems (Transducers '05) (Seoul, Korea, 5–9 June)* vol 2, pp 1525–8

[41] Ekstrand G and Thorsén G Liquid router *Patent Application* US20050141344A1 (Gyros AB)

[42] Brenner T, Glatzel T, Zengerle R and Ducrée J 2005 Frequency-dependent transversal flow control in centrifugal microfluidics *Lab on a Chip* **5** 146–50

[43] Haeberle S, Naegele L, Zengerle R and Ducrée J 2006 A digital centrifugal droplet-switch for routing of liquids *Proc. 10th Int. Conf. on Miniaturized Systems for Chemistry*

and Life Sciences (μTAS2006) (Tokyo, Japan, 5–9 Nov.) vol 1, ed H Fujita, T Kitamori and S Hasebe (Society for Chemistry and Micro-Nano Systems) pp 570–2

[44] Haeberle S, Schmitt N, Zengerle R and Ducrée J 2007 Centrifugo-magnetic generation of gas-liquid microflows *Sensors Actuators* A **135** 28–33

[45] Jackson W C, Tran H D, O'Brien M J, Rabinovich E and Lopez G P 2001 Rapid prototyping of active microfluidic components based on magnetically modified elastomeric materials *J. Vac. Sci. Technol.* B **19** 596–9

[46] Haeberle S, Zengerle R and Ducrée J 2007 Centrifugal generation and manipulation of droplet emulsions *Microfluid. Nanofluid.* **3** 65–75

[47] Haeberle S, Naegele L, Burger R, Zengerle R and Ducrée J 2007 Alginate micro-bead fabrication on a centrifugal microfluidics platform *Proc. 20th IEEE Int. Conf. on Micro Electro Mechanical Systems (MEMS 2007) (Kobe, Japan, 21–25 Jan.)* (IEEE) pp 497–500

[48] Riegger L, Grumann M, Steigert J, Zengerle R and Ducrée J 2006 Microfluidics on a conventional, 10-$ CDROM drive: all-in-one determination of the hematocrit *Proc. 10th Int. Conf. on Miniaturized Systems for Chemistry and Life Sciences (μTAS2006) (Tokyo, Japan, 5–9 Nov.)* vol 2, ed H Fujita, T Kitamori and S Hasebe (Sapporo, Japan: Society for Chemistry and Micro-Nano Systems) pp 1555–7

[49] Riegger L *et al* 2007 Single-step centrifugal hematocrit determination on a 10-$ processing device *Biomed. Microdev.* at press

[50] Haeberle S, Brenner T, Zengerle R and Ducrée J 2006 Centrifugal extraction of plasma from whole blood on a rotating disk *Lab on a Chip* **6** 776–81

[51] Ramos A, Morgan H, Green N G and Castellanos A 1998 AC electrokinetics: a review of forces in microelectrode structures *J. Phys. D: Appl. Phys.* **31** 2338–53

[52] Hughes M P 2002 Strategies for dielectrophoretic separation in laboratory-on-a-chip systems *Electrophoresis* **23** 2569–82

[53] Gascoyne P R C and Vykoukal J 2002 Particle separation by dielectrophoresis *Electrophoresis* **23** 1973–83

[54] Boettcher M, Jaeger M S, Riegger L, Ducrée J, Zengerle R and Duschl C 2006 Lab-on-chip-based cell separation by combining dielectrophoresis and centrifugation *Biophys. Rev. Lett.* **1** 443–51

[55] Steigert J, Haeberle S, Müller C, Steinert C P, Gottschlich N, Reinecke H, Rühe J, Zengerle R and Ducrée J 2007 Rapid prototyping of microfluidic chips in COC *J. Micromech. Microeng.* **17** 333–41

[56] McDonald J C, Duffy D C, Anderson J R, Chiu D T, Wu H, Schueller O J A and Whitesides G M 2000 Fabrication of microfluidic systems in poly(dimethylsiloxane) *Electrophoresis* **21** 27–40

[57] Becker H and Gärtner C 2000 Polymer microfabrication methods for microfluidic analytical applications *Electrophoresis* **21** 12–26

[58] Brenner T, Gottschlich N, Knebel G, Mueller C, Reinecke H, Zengerle R and Ducrée J 2005 Injection molding of microfluidic chips by epoxy-based master tools *Proc. 9th Int. Conf. on Miniaturized Systems for Chemistry and Life Sciences (μTAS 2005) (Boston, MA, 9–13 Oct.)* ed K F Jensen, J Han, D J Harrison and J Voldman pp 193–5

[59] Menz W 1996 LIGA and related technologies for industrial application *Sensors Actuators* A **54** 785–9

[60] Lutz S, Grumann M, Gutmann O, Dube M, Riegger L, Steigert J, Müller C, Daub M, Zengerle R and Ducrée J 2006 Centrifugal processor for standard microarray slides *Proc. 10th Int. Conf. on Miniaturized Systems for Chemistry and Life Sciences (μTAS2006) (Tokyo, Japan, 5–9 Nov.)* vol 1, ed H Fujita, T Kitamori and S Hasebe (Society for Chemistry and Micro-Nano Systems) pp 329–31

[61] Grumann M, Steigert J, Riegger L, Moser I, Enderle B, Urban G, Zengerle R and Ducrée J 2006 Sensitivity enhancement for colorimetric glucose assays on whole blood by on-chip beam-guidance *Biomed. Microdev.* **8** 209–14

[62] Steigert J, Grumann M, Brenner T, Riegger L, Harter J, Zengerle R and Ducrée J 2006 Fully integrated whole blood testing by real-time absorption measurement on a centrifugal platform *Lab on a Chip* **6** 1040–1044

[63] Bundgaard F, Geschke O, Zengerle R and Ducrée J A simple opto-fluidic switch detecting liquid filling in polymer-based microfluidic systems *Transducers '07 Conf. (Lyon, France, 10–14 June)* at press

[64] Steigert J *et al* 2005 Integrated sample preparation, reacting and detection on a high-frequency centrifugal microfluidic platform *J. Assoc. Lab. Autom.* **10** 331–41

[65] Steigert J, Grumann M, Dube M, Streule W, Riegger L, Brenner T, Koltay P, Mittmann K, Zengerle R and Ducrée J 2006 Direct hemoglobin measurement on a centrifugal microfluidic platform for point-of-care diagnostics *Sensors Actuators* **A 130–131** 228–33

[66] Riegger L, Steigert J, Grumann M, Lutz S, Olofsson G, Khayyami M, Bessler W, Mittenbuehler K, Zengerle R and Ducrée J 2006 Disk-based parallel chemiluminescent detection of diagnostic markers for acute myocardial infarction *Proc. 10th Int. Conf. on Miniaturized Systems for Chemistry and Life Sciences (μTAS2006) (Tokyo, Japan, 5–9 Nov.)* vol 1, ed H Fujita, T Kitamori and S Hasebe (Society for Chemistry and Micro-Nano Systems) pp 819–21

[67] Grumann M, Dobmeier M, Schippers P, Brenner T, Kuhn C, Fritsche M, Zengerle R and Ducrée J 2004 Aggregation of bead-monolayers in flat microfluidic chambers—simulation by the model of porous media *Lab on a Chip* **4** 209–13

[68] Riegger L *et al* 2005 Read-out concept for multiplexed bead-based fluorescence immunoassays on centrifugal microfluidic platforms *Sensors Actuators* A **126** 455–62

[69] Grumann M, Riegger L, Nann T, Ehlert O, Mittenbühler K, Urban G, Pastewka L, Brenner T, Zengerle R and Ducrée J 2005 Parallelization of chip-based fluorescence immunoassays with quantum-dot labelled beads *Proc. 13th Int. Conf. on Solid-State Sensors, Actuators & Microsystems (Transducers '05) (Seoul, Korea, 5–9 June)* vol 2, pp 1114–7

[70] Grumann M, Brenner T, Beer C, Zengerle R and Ducrée J 2005 Visualization of flow patterning in high-speed centrifugal microfluidics *Rev. Sci. Instrum.* **76** 025101